



American  
Gear Manufacturers  
Association

19FTM02

## **AGMA Technical Paper**

# Misalignment Compensation Spline Design

By Dr. Davide Marano, Mariano Lorenzini, Luca Mastrandrea, Francesco Pulvirenti, Ferrari Auto, Dr. Massimiliano Turci, Studio Tecnico Turci, and Nicolas Fillault, INSA Lyon

# Misalignment Compensation Spline Design

**Dr. Davide Marano, Mariano Lorenzini, Luca Mastrandrea, Francesco Pulvirenti,  
Dr. Massimiliano Turci, and Nicolas Fillault, M.Sc.**

[The statements and opinions contained herein are those of the author and should not be construed as an official action or opinion of the American Gear Manufacturers Association.]

## Abstract

Shaft misalignment is a significant problem in the design of spline joint transmissions. Involute splines with flank line crowned teeth are a solution to compensate shaft parallel misalignments avoiding interferences between shaft and hub teeth. A precise determination of the influence of misalignment on spline load capacity can be performed by FEM or other powerful numerical simulation.

In this study a geometrical model of crowned spline joint for misalignment compensation is proposed. Flank line crowning is determined as a function of shaft misalignment and the minimum theoretical circumferential backlash.

The proposed approach is adopted for the design of a spline joint, part of a high-performance automotive driveline. Finite element simulation has been performed to determine the spline loaded tooth contact pattern and optimize the theoretical crowning value. Experimental results are in good agreement with simulations.

Keywords: Power transmission, Spline joint, Misalignment, Crowning, Pitch deviation, Analytical modelling, Concentration factor, Strength calculations.

Copyright © 2019

American Gear Manufacturers Association  
1001 N. Fairfax Street, Suite 500  
Alexandria, Virginia 22314

October 2019

ISBN: 978-1-64353-041-3

# Misalignment Compensation Spline Design

**Dr. Davide Marano, Mariano Lorenzini, Luca Mastrandrea, Francesco Pulvirenti, Ferrari Auto, Dr. Massimiliano Turci, Studio Tecnico Turci, and Nicolas Fillault, M.Sc., INSA Lyon**

## 1 Introduction

Spline joints are commonly used in power transmission systems to provide torque and speed from a shaft to its hub and vice versa, preventing movements in a peripheral direction. A spline coupling has a higher load capacity than a conventional keyed shaft, resulting from its multiple teeth. Moreover, they allow a certain amount of parallel and angular misalignment among connected shafts and relative sliding between shaft and hub. Spline teeth can be straight-sided or have involute profile forms (Figure 1).



**Figure 1 – Spline joints (Courtesy of CIMA S.p.A.)**

### 1.1 Geometry Standards

Involute splines can be seen as a gear with special profile in line with international and national regulations. The Society of Automotive Engineers (SAE) has published the ANSI B92.1 standard. The last edition is [1], approved by the American National Standards Institute, as a result of a joint effort by the “SAE Involute Splines, Serrations and Inspection Committee” and “ANSI Standards Committee B92”, reporting design and inspection guidelines for involute splines. The American Gear Manufacturers Association (AGMA) has recently published AGMA 945-A18 Information Sheet [2], covering parallel straight sided and involute splines. This document provides state of the art information about geometry, fit types, materials, manufacturing, rating, inspection, lubrication, and failure of splined elements. Some details of spline couplings design guidelines are presented in ANSI/AGMA 6123-C16 [3].

The International Organization for Standardization (ISO) has released in 2005 the last edition of the ISO 4156 international standard [4], providing the data and the necessary indications for the design (ISO 4156-1), manufacture (ISO 4156-2) and inspection (ISO 4156-3) of straight (non-helical) side-fitting cylindrical involute splines. The involute splines in accordance with ISO 4156 are based on series of modules and the nominal pressure angles are  $30^\circ$ ,  $37,5^\circ$  and  $45^\circ$ ; these are not interchangeable.

The Deutsches Institut für Normung (DIN) has published in 2006 the last edition of the DIN 5480 standard [5], which deals with involute splines and interacting involute splines. This standard is based on reference diameters that are independent from the module. This makes possible to adapt the gears to standardized ball and roller bearing diameters and to reduce the number of different loads required for manufacturing. The DIN 5480 serie of standards is limited to splines with a pressure angle of  $30^\circ$  and comprises guidelines for design (DIN 5480-1), nominal dimensions and inspecting dimensions (DIN 5480-2), quality inspection (DIN 5480-15) and tools (DIN 5480-16).

The Association Française de Normalisation (AFNOR) has released in 1955 the NF E22-141 standard [6], to specify and explain the principles for designing and producing straight splines with involute sides, in accordance with the same techniques and the same machine tools as for producing gear teeth. In the AFNOR E22-148 standard [7], tolerances related to splines and methods of inspection are presented.

The Italian association CUNA (Commissione Tecnica di Unificazione nell’Autoveicolo), a UNI (Ente nazionale italiano di unificazione) federation, has released in 1955 the CUNA B129 standard, reporting design tables for straight splines with involute sides. These tables are actually reported in the mechanical designer handbook [8].

## 1.2 Strength Calculation

During power transmission spline like gear teeth are subjected to stresses in bending, shear, compressive and contact loads. A milestone in the spline design and diagnosis of spline-failure problems is the work of D.W. Dudley [9,10,11]. In his work Dudley identifies five possible failure modes of spline teeth and supplies charts and formulas for computing shear stresses in spline shaft, shear stresses in spline teeth, compressive stresses in spline teeth and bursting stresses in internal spline parts.

For as concerns design formulas proposed by Niemann [12], the equation for calculating the mean pressure between teeth in an involute spline coupling is:

$$p = \frac{T}{z L h_w R_m} k_{\phi\beta} k_l \quad (1)$$

where

$p$  is the contact pressure (no crowning radius is taken into account in this approach);

$T$  is the applied torque;

$k_{\phi\beta}$  and  $k_l$  are respectively the load sharing and longitudinal factors.

The pressure value  $p$  (that can be calculated either from maximum, nominal or equivalent torque) has to be compared to the admissible pressure related to the material characteristics. In general, the admissible pressure is obtained by static characterization of the material, corrected by parameters or safety factors related to the required number of cycles [22].

## 1.3 Crowned Splines

Crowned-teeth splines are introduced in [9] as a solution to handle shaft misalignments and a misalignment factor ( $K_m$ ) is proposed to account for how misalignment affects spline stress. An analytical study using Spline LDP, a quasi-static load distribution program for splines created by GearLab (Ohio State University), has been recently presented by McKenny [13], to check whether splines with a range of diameters exhibit the same pattern of misalignment load factor vs. face width that Dudley published in [9]. Results showed that the misalignment load factors slope is dependent on the length/diameter (L/D) ratio of the spline: splines with a L/D ratio of 1.0 follow a power function slope, splines with L/D ratio 0.2 are nearly linear over the studied range. An iterative calculation method, non-finite element method based to determine both the exact number of engaging teeth and shared forces in involute spline couplings with parallel offset errors is reported in the works of Curà [14,15]. Both semi-analytic approach and finite elements method have been extensively applied by Hong et al. [16-17-18] to investigate the effect of spline misalignment along with intentional lead crowning of contacting surfaces and effects of manufacturing tooth indexing errors on spline load distribution. A comparison between analytical and experimental study results for the load distribution on the length of joints under pure torque is presented in [19].

A novel spline coupling test rig has been developed by Mura [20-22]; its peculiarity is to allow angular misalignments between hub and shaft in order to investigate the behavior of spline couplings in real working conditions, in particular to investigate fretting wear phenomena. The fretting behavior of misaligned splines has been studied also by Medina [24-26]. In [25] approximate formulas are provided in order to describe the pressure and wear behavior of the coupling in terms of dimensionless parameters. In [27] a relation to calculate the optimal spline crowning is presented.

This paper aims at developing guidelines for the design of involute splines for misalignment compensation. The objectives of this paper are as follows:

- develop a geometrical model of a crowned spline joint to compensate a given shaft misalignment;
- present an industrial case study of a crowned spline joint designed to withstand a given misalignment. Both analytical and FEM based results are compared with experimental evidences.

## 2 Crowned Spline Design for Misalignment Compensation

The modelling of crowned spline joint is introduced and a relation to determine minimum crowning to compensate a given shaft misalignment compensation is derived in this section.

The reference systems are shown in Figure 2 and Figure 3: the *global* reference system ( $O_cSVX$ ) is defined on the base cylinder axis, the *local* reference system ( $Oxyz$ ) related to a tooth, is shifted from the global reference by a value close to the pitch radius  $r$  in the  $z$  direction.

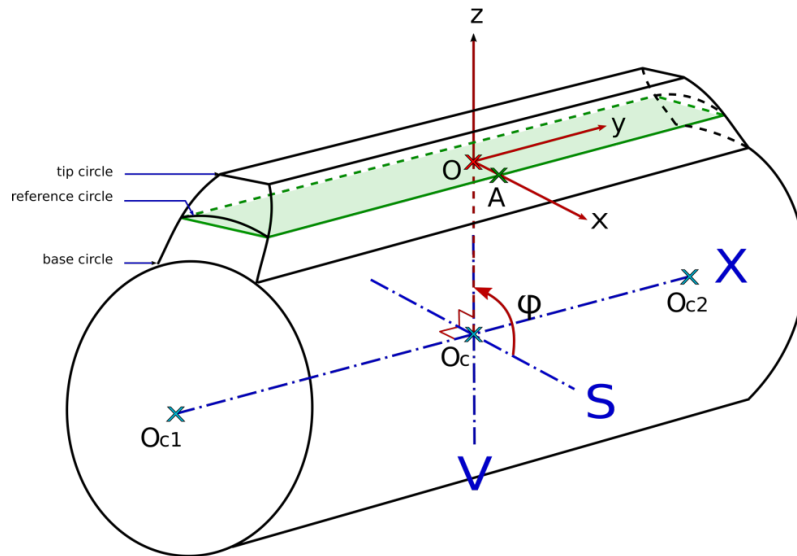


**Figure 2 – Spline shaft global reference system and basic notation**

The position of the considered tooth is identified with respect to the axis  $S$  by means of the angle  $\varphi$  (Figure 2).

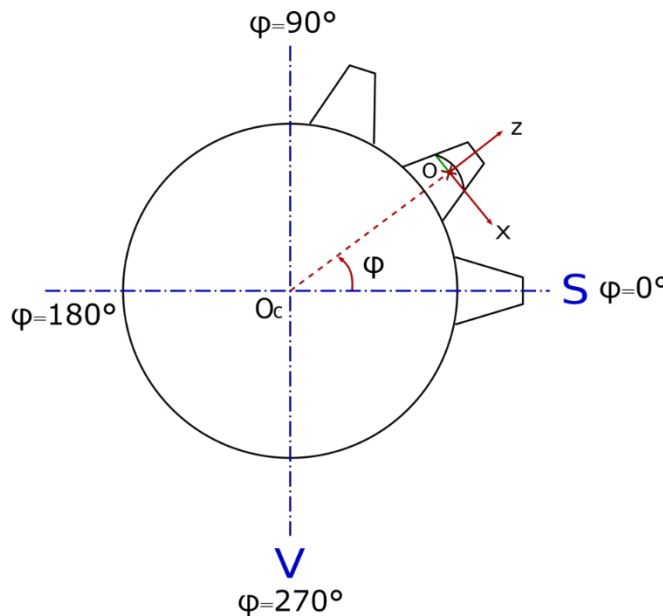


**Figure 3 – Spline shaft local reference system**

Spline joints are used to couple shafts rotation and tooth flank line crowning allows to compensate for parallel misalignment of shafts. As defined in ISO 21771 [28], tooth flank line crowning  $C_\beta$ , is the continuously increasing of the flank line from a common defined point of the main geometry, symmetrically in the direction of both ends of the tooth (arc-shaped or parabolic), as shown in Figure 4.

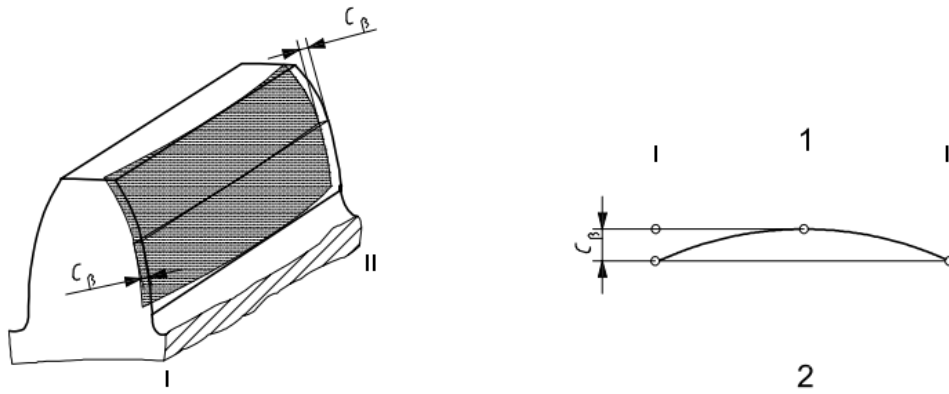


**Figure 4 – Spline tooth flank crowning**

Flank line crowning is usually applied only to the external spline (shaft) due to manufacturing capabilities. Between hub and shaft there is commonly a difference of 1 point of accuracy (quality). Small pieces could be produced by spark erosion (EDM) either with a solid electrode or by wire cutting.

Basic geometrical and misalignment parameters of either single and double spline joints are introduced in Figure 5 and Figure 6; shaft teeth crowning is considered. With reference to Figure 5 and Figure 6,  $X_1$  is the normal axis of the shaft,  $X_2$  is the normal axis of the hub,  $b$  is the spline face width,  $r_c$  is the crowning radius (usually equal to the reference radius, but it can be different),  $\rho$  is the transverse crowning radius and  $\theta$  is the misalignment angle. The misalignment angle  $\theta$  results from the parallel shaft misalignment in a double spline joint as illustrated Figure 5, as follows:

$$\theta = \arcsin\left(\frac{V}{L}\right) \quad (2)$$

where

$L$  is the useful length and  $V$  is the parallel shaft misalignment.

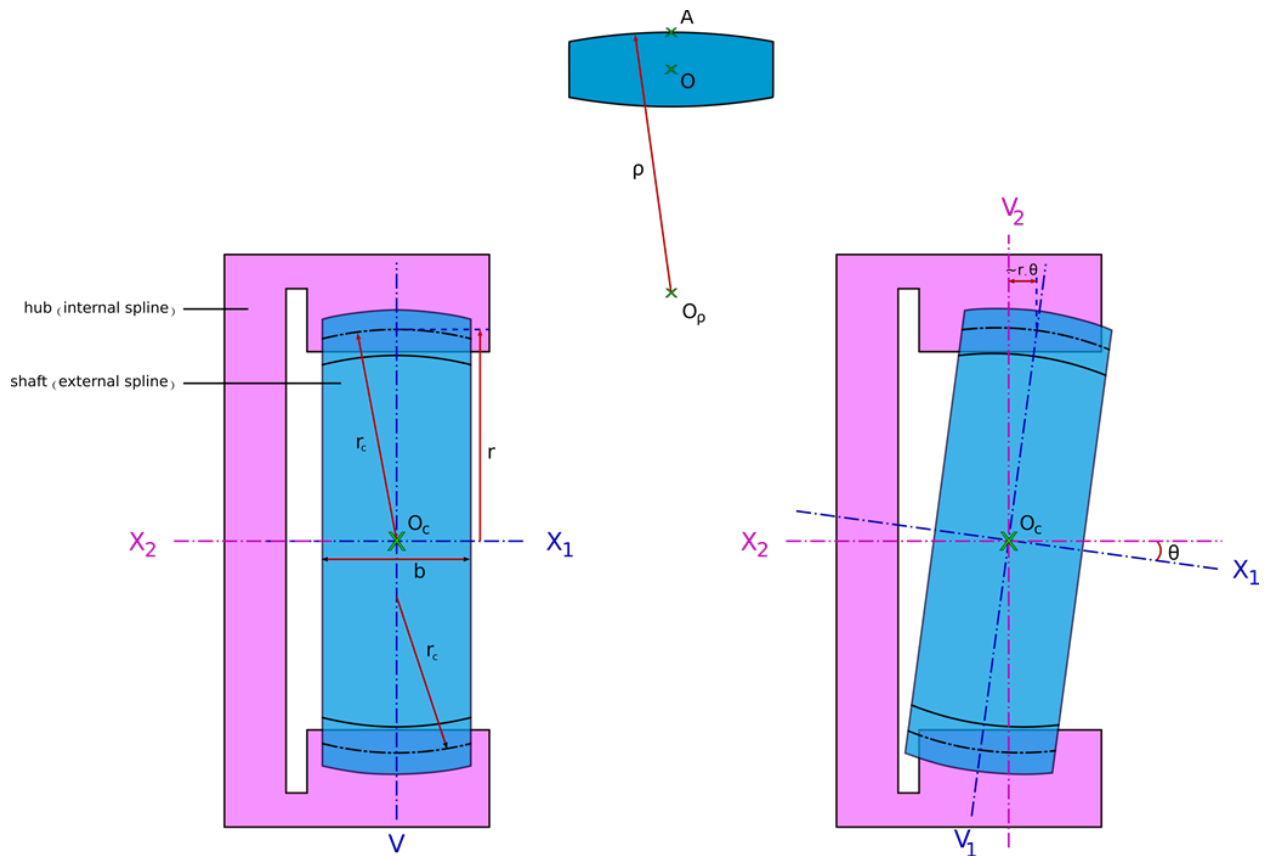


Figure 5 – Basic geometrical parameters and misalignment– Single Spline Joint

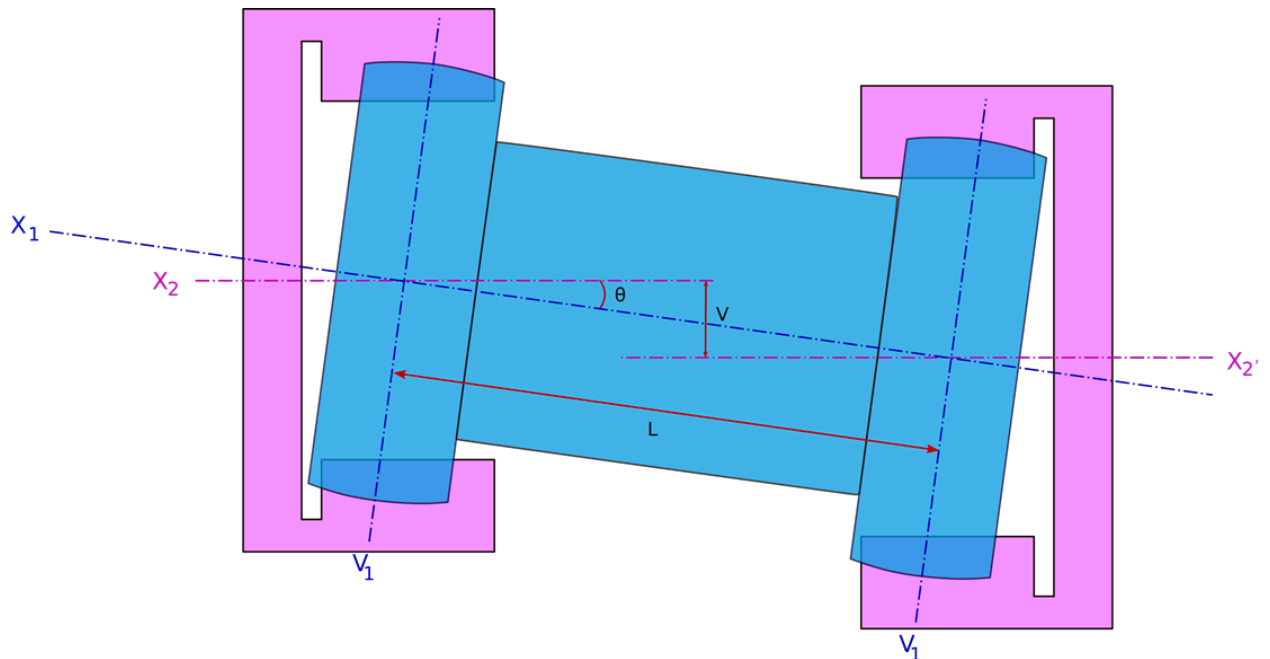


Figure 6 – Basic geometrical parameters and misalignment – Double Spline Joint

## 2.1 Spline Backlash and Misalignment

In the following the different circumferential backlash parameters  $J_t$ ,  $j_t$  and  $j_a$  are introduced. The total circumferential backlash  $J_t$  (Figure 7A), chosen during the spline design, is the theoretical total backlash depending on the selected tolerance class. The effective backlash  $j_t$  (Figure 7B), is defined as the

circumferential backlash resulting from the misalignment angle  $\varepsilon$  ( $\varepsilon=\theta$  for  $\varphi=0$ ). The value of the effective backlash  $j_t$  thus depends on the position  $\varphi$  of the considered shaft tooth and on the chosen circumferential backlash  $J_t$ . The actual backlash is  $j_a$  (Figure 7B) and is considered regarding the active flank. Either the right or the left flank of the shaft tooth could be the active flank. Following has been supposed that no load is applied, thus some geometrical considerations have been assumed e.g.,  $j_a$  equal to the half of  $j_t$ .

The angle  $\varepsilon$  is defined as the tilt angle around the z axis due to a misalignment  $\theta$  and corresponds to the offset angle between  $(Oxy)$  and  $(O'x'y')$ , as shown in Figure 7B:

$$\begin{aligned} \varepsilon &\cong \theta \text{ for } \varphi = 0^\circ, \varphi = 90^\circ; \\ \varepsilon &\cong \theta \cos \varphi \text{ for } \varphi \in ]0^\circ, 90^\circ[ \end{aligned} \quad (3)$$

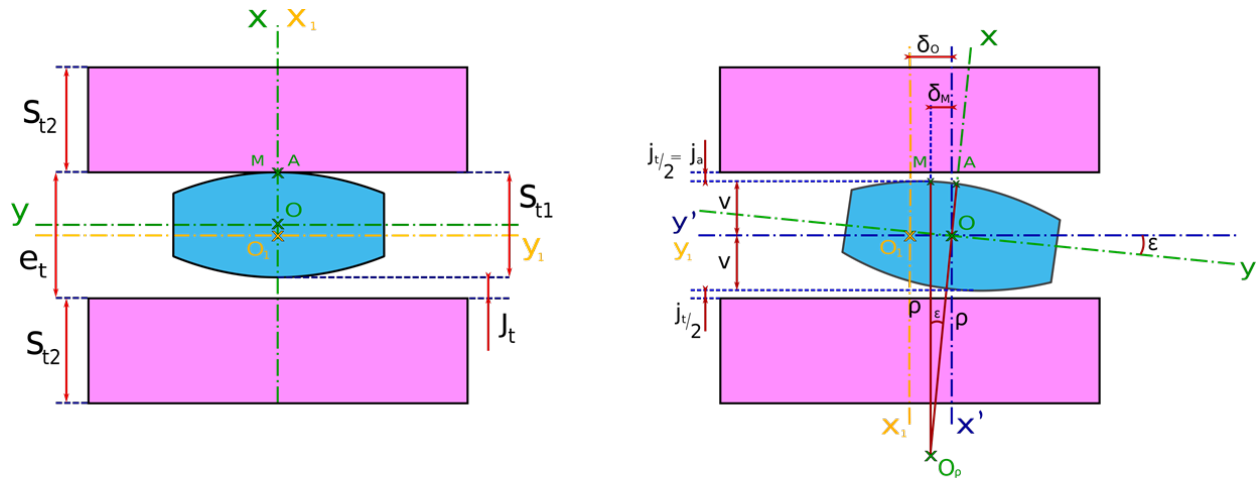


Figure A

Figure B

Figure 7 – Spline teeth meshing

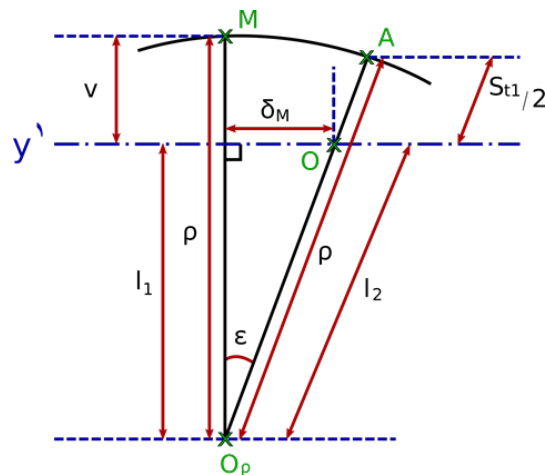


Figure 8 – Teeth spline meshing (detail of Figure 7B)

With regard to Figure 8, the point M is the contact point between the active flank of the shaft tooth and the facing hub tooth, the point A is the apex point of the crowned shaft tooth flank. The length  $v$  is defined as the y coordinate of the contact point M:

$$v = \rho - l_1 \quad (4)$$



since  $\cos \varepsilon = \frac{l_1}{l_2}$  and  $l_2 = \rho - \frac{S_{t1}}{2}$  then substituting in equation 2 one has:

$$v = \rho - \left( \rho - \frac{S_{t1}}{2} \right) \cos \varepsilon \quad (5)$$

With reference to Figure 7, the effective backlash  $j_t$  can be expressed as a function of the total circumferential backlash as:

$$j_t = J_t + S_{t1} = 2v \quad (6)$$

by simple algebraic manipulation one has:

$$j_t = J_t + (1 - \cos \varepsilon) (S_{t1} = 2\rho) \quad (7)$$

As the transverse crowning radius  $\rho$  is much bigger than the other spline parameters,  $\rho \gg S_{t1}$ . The Gauss approximation can be applied to the cosine trigonometric function in the previous equation:  $\cos \varepsilon \cong 1 - \frac{\varepsilon^2}{2}$ .

The effective transverse backlash  $j_t$  is then:

$$j_t = J_t = \rho \theta^2 \cos^2 \varphi \quad (8)$$

Equation (8) provides the relation between the transverse backlash  $J_t$  and the misalignment  $\theta$ .

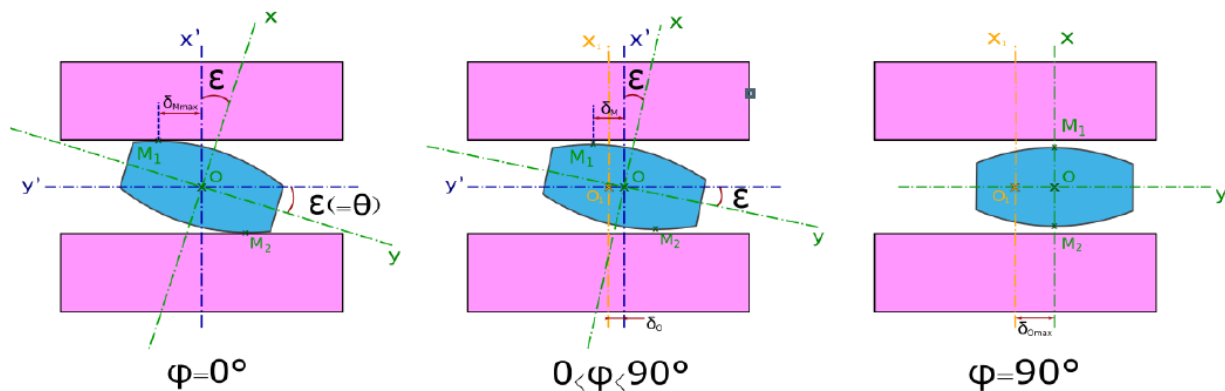


Figure 9 – Relative spline joint teeth position

### 2.1.1 Transverse Backlash $J_t$ for $\varphi=0^\circ$

For a hinge tooth (teeth with  $\varphi=0^\circ$  or  $180^\circ$ ), equation (8) becomes:

$$j_t = J_t = \rho \theta^2 \quad (9)$$

As shown in Figure 9, in this case, two flanks of the shaft tooth are in contact with the hub teeth if  $J_t = \rho \theta^2$ :

$$J_{t \min} = \rho \theta^2; \rho_{\max 1} = \frac{J_t}{\theta^2} \quad (10)$$

Equation (10) gives the minimum backlash  $J_{t \min}$  to compensate a given misalignment  $\theta$  in the design of a crowned spline.

### 2.1.2 Actual Backlash $j_a$ for $0 < \varphi < 90^\circ$ and $J_t = J_{\min}$

Considering  $J_t = J_{\min}$ , from equation (8) and (10) one has:

$$j_t = \rho \theta^2 \sin^2 \varphi \quad (11)$$

Since  $J_t = J_{min}$  as shown in Figure 7B  $j_t = 2j_a$ , giving:

$$j_a = \frac{1}{2} \rho \theta^2 \sin^2 \varphi \quad (12)$$

## 2.2 Spline Face Width and Misalignment

The misalignment has an influence on the position of the contact point M on the active flank of the shaft tooth as shown in Figure 9. Since the theoretical contact point M has to correspond with a real point located on the active flank of the hub tooth, the contact point displacement,  $\delta_M$ , must be:

$$\delta_{Mmax} = b_{min\ hub} / \theta^2 \quad (13)$$

The contact point displacement  $\delta_M$  is given, as shown in Figure 8, by:

$$\delta_M = (\rho - v) \tan \varepsilon \quad (14)$$

Substituting equation (5) in (14) and considering gauss approximations of cosine and tangent trigonometric functions one has:

$$\begin{aligned} \delta_M &= \rho \varepsilon \\ \delta_M &= \rho \theta \cos \varphi \end{aligned} \quad (15)$$

As shown in Figure 9 and according to the equation (17), the maximum contact point displacement  $\delta_{Mmax}$  is obtained on the hinge teeth (teeth orientation  $\varphi = 0^\circ$ ), thus:

$$\delta_{Mmax} = \rho \theta \quad (16)$$

Combining equation (15) in (16) the minimum spline face width is given by  $b_{min\ hub} = 2\rho \cdot \theta$  and the crowning radius can be expressed as a function of shaft misalignment and spline face width as:

$$\rho_{max2} = \frac{b_{hub}}{2\theta} \quad (17)$$

## 3 Determination of Flank Line Crowning ( $C_\beta$ )

Below is derived the relation among the flank line crowning  $C_\beta$  and the given shaft misalignment to compensate  $\theta$ . Three different sections of a crowned shaft tooth are shown in Figure 10.

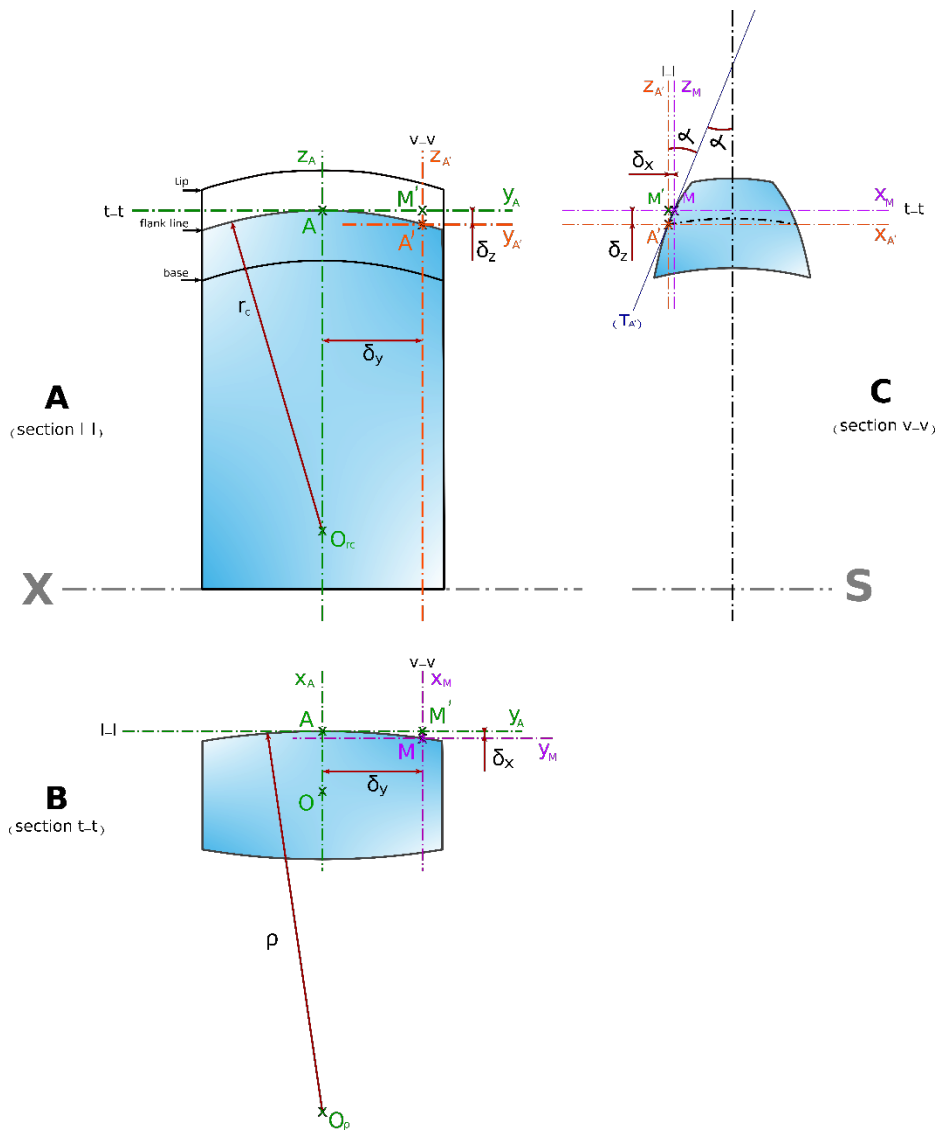


Figure 10 – Parametric representation of spline tooth face

In the following Table 1 the parameters related to Figure 10 are listed and explained.

**Table 1 – Parameters related to Figure 10**

<b>Section Planes</b>	
<b>Name</b>	<b>Description</b>
(l-l)	Plane defined by $z_{A'}$ and $y_A$ , perpendicular to the horizontal plane and crossing the flank line. The longitudinal section (section l-l) represents a tooth flank. The addendum flank is not visible since the plane (l-l) is not oriented by the surface tooth shape
(t-t)	Plane defined by $y_{A'}$ and $x_M$ , parallel to the horizontal plane and crossing the point A. The line defined by the intersection of (t-t) and (l-l) could be assimilated to the theoretical flank line without crowning. The transverse section shows a top flank of the tooth at the reference circle
(v-v)	Plane defined by $z_{A'}$ and $x_M$ , perpendicular to the horizontal plane and crossing any point M. The vertical section shows a datum face
<b>Marks, axes and useful points</b>	
<b>Name</b>	<b>Description</b>
( $A_{x_A y_A z_A}$ )	Tooth reference mark
( $A'_{x_{A'} y_{A'} z_{A'}}$ )	Mark relative to the point A' (this point is described below). ( $A'_{x_{A'} y_{A'} z_{A'}}$ ) is offset from ( $A_{x_A y_A z_A}$ ) by the distances $\delta_z$ and $\delta_y$ introduced hereafter
( $M_{x_M y_M z_M}$ )	Mark relative to the point M (this point is described below). ( $M_{x_M y_M z_M}$ ) is offset from ( $A_{x_A y_A z_A}$ ) by the distances $\delta_y$ and $\delta_x$ introduced hereafter
X	Normal axis of the gear (cylinder)
S	"Hinge axis" in Figure 10, axes S and X are transparent because there are supposed not being visible on this section.
A	Apex point of the shaft tooth flank and middle of the flank line. That means, A is the theoretical point of contact ( $A = M$ )
A'	Arbitrary point located on the flank line
M	Arbitrary point located on the surface of the crowned flank
M'	Projection of the point M on the $y_A$ axis. It corresponds to the theoretical position of the point M without transverse crowning
$T_{A'}$	Tangent line at the point A'
$O_{rc}$	Origin of the crowning radius $r_c$
$O_p$	Origin of the transverse crowning radius $\rho$
<b>Displacements of interest</b>	
<b>Symbol</b>	<b>Description</b>
$\delta_x$	Transverse distance between the point A and the point M. It corresponds to the reduction of the half tooth section (t-t).
$\delta_y$	Axial distance between the chosen point M and the middle of the tooth
$\delta_z$	Radial distance between the points M' and A'. In some ways, it corresponds to the displacement of the flank line owing to the crowning

According to Figure 10, the following geometrical relationship can be written:

$$\delta_y^2 = 2\delta_z r_c + \delta_z^2 \quad (18)$$

It is possible to approximate equation (18) considering that  $\delta_z^2 \ll 2\delta_z r_c$  as:

$$\delta_y^2 = 2\delta_z r_c \quad (19)$$

According to Figure 10,  $\delta_x = \delta_z \tan \alpha$ , then:

$$\delta_y^2 = 2 \frac{r_c}{\tan \alpha} \delta_x \quad (20)$$

It is possible to obtain  $\delta_y$  as a function of  $\delta_x$  and  $\rho$  in Figure 10 as follows:

$$\delta_y^2 = 2 \delta_x \rho + \delta_x^2 \quad (21)$$

It is possible to approximate equation (21) considering  $\delta_x^2 \ll 2 \delta_x \rho$ :

$$\delta_y^2 = 2 \delta_x \rho \quad (22)$$

Combining equations 20 and 22 one has the algebraic relation among the transverse crowning radius  $\rho$  and the crowning radius  $r_c$ :

$$2 \frac{r_c}{\tan \alpha} \delta_x = 2 \delta_x \rho \quad (23)$$

$$\rho = \frac{r_c}{\tan \alpha}$$

The flank line crowning can be considered as a parabola of equation  $y^2 = 2 p x$  with:  $p = \rho = \frac{r_c}{\tan(\alpha)}$ . The equation can be rewritten as a function of  $\delta_{y_{max}}$  and  $\delta_{x_{max}}$  as:

$$\delta_{y_{max}}^2 = 2 \rho \delta_{x_{max}}$$

$$\left(\frac{b}{2}\right)^2 = 2 \rho C_\beta \quad (24)$$

$$C_\beta = \frac{b^2}{8 \rho}$$

The relationship among the crowning  $C_\beta$  and the given shaft misalignment  $\theta$  to compensate is obtained substituting equation 17 in equation 24, leading to:

$$C_\beta = \frac{\theta b}{4} \quad (25)$$

#### 4 Case Study

The theory presented in Section 2 has been applied to design a spline for high performance automotive driveline application. This spline must compensate a given amount of shaft misalignment and withstand high internal combustion engine torque.

In Figure 11 the FEM analysis of the shaft spline with no flank line crowning is shown. A stress concentration is detected at the edge of the spline face width, that must be avoided. In order to prevent the “butfress effect” a flank line crowning is applied to the spline according to equation (25), considering the maximum geometrical shaft misalignment  $\theta_{max}$ .

The FEM analysis of the crowned teeth spline is shown in Figure 12: the contact is well distributed along the face width and no stress concentration is detected. An optimization of the crowning value has then been performed by means of multiple finite element analysis simulations.

In Figure 12 the spline joint is shown after wear test, confirming the effectiveness of the FEM loaded tooth contact pattern.

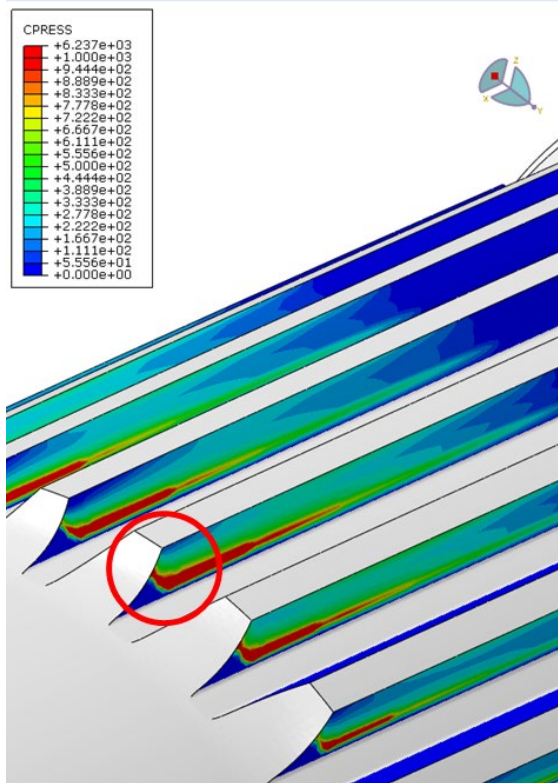


Figure 11 – Spline joint with no crowning

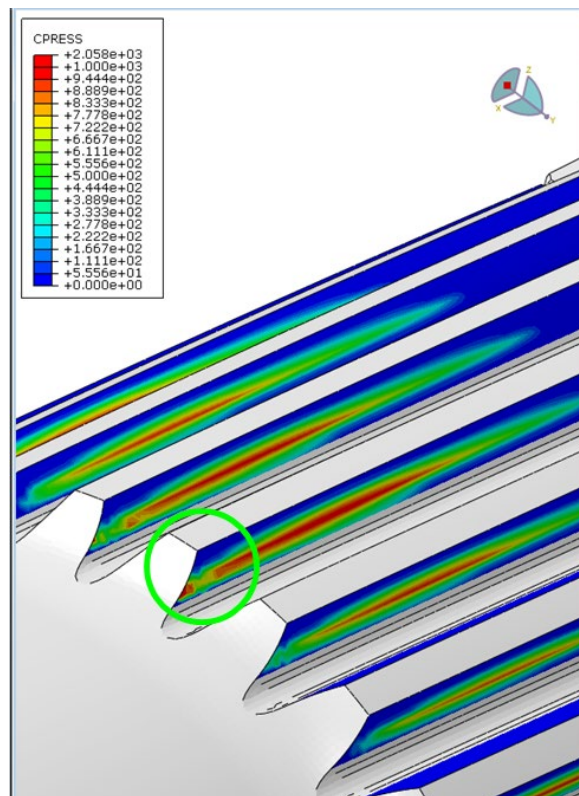
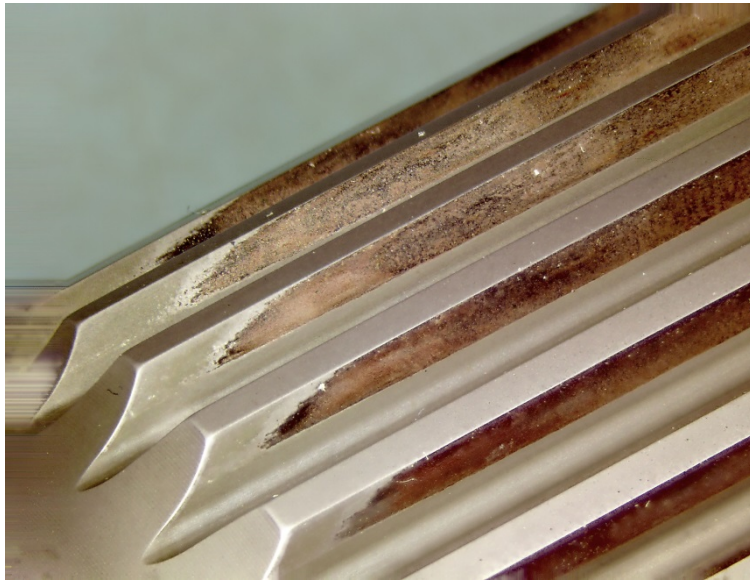


Figure 12 – Spline joint with crowning



**Figure 13 – Spline joint contact pattern**

## **5 Conclusion**

In this paper a method to design crowned splines for shaft misalignment compensation has been presented. A geometrical relationship among the flank line crowning and the shaft misalignment is provided.

The proposed approach has been adopted for the design a spline joint, part of a high-performance automotive driveline. Finite element simulation has been performed to determine the spline loaded tooth contact pattern and optimize the crowning value. Experimental results are in good agreement with simulations.

## **Acknowledgment**

The authors would like to thank Maurizio Corsellini (CIMA S.p.A.) for providing spline figures; KissSoft AG (a Gleason Company) for the support in the calculation of the splined joint according to several standards and in the generation of the crowned 3D model.

## Bibliography

- [1] STANDARD ANSI B92.1-1996, “*Involute Splines and Inspection*”, *Society of Automotive Engineers*
- [2] AGMA 945-A18, “*Splines – Design and Application*”
- [3] ANSI/AGMA 6123-C16, “*Design Manual for Enclosed Epicyclic Gear Drives*”
- [4] ISO 4156, 2005, “*Straight cylindrical involute splines – Metric module, side fit – Part 1: Generalities, Part 2- Dimensions, Part 3- Inspection*”
- [5] DIN 5480, 2006 “*Splined connections with involute splines based on reference diameters – Part 1: Principles*”
- [6] AFNOR NF E22-141, “*Cylindrical involute splines.*”
- [7] AFNOR E22.148, “*Straight cylindrical involute splines – Dimensional selection and verification*”
- [8] Baldassini, L. (2014). *Vademecum per disegnatori e tecnici*, Hoepli
- [9] Dudley, D.W., 1957, “*When splines need stress control,*” *Prod. Engineering*, vol. no. 28, pp. 56-59
- [10] Dudley, D.W., 1957, “*How to design involute splines,*” *Prod. Engineering*
- [11] Dudley D.W., *Dudley’s Gear Hand Book*. 2nd Edition, McGraw-Hill, Inc., 1991.
- [12] Niemann, G., Winter, H., Höhn, B. R. (1982,1990,2002,2005). *Maschinenelemente Band I-IV Auflage*. Springer-Verlag Berlin Heidelberg New York.
- [13] S. McKenny, *Filling some gaps in spline design guidelines: Centering, Friction and Misalignment* (2018), AGMA Technical Fall Meeting
- [14] Cuffaro, V., Cura, F., & Mura, A. (2012). Analysis of the pressure distribution in spline couplings. *Proceedings of the Institution of Mechanical Engineers, Part C: Journal of Mechanical Engineering Science*, 226(12), 2852-2859
- [15] Cura, F., Mura, A., & Gravina, M. (2013). Load distribution in spline coupling teeth with parallel offset misalignment. *Proceedings of the Institution of Mechanical Engineers, Part C: Journal of Mechanical Engineering Science*, 227(10), 2195-2205.
- [16] Hong, J., Talbot, D., & Kahraman, A. (2014). Load distribution analysis of clearance-fit spline joints using finite elements. *Mechanism and Machine Theory*, 74, 42-57.
- [17] Hong, J., Talbot, D., & Kahraman, A. (2014). A semi-analytical load distribution model for side-fit involute splines. *Mechanism and Machine Theory*, 76, 39-55.
- [18] Hong, J., Talbot, D., & Kahraman, A. (2015). Effects of Tooth Indexing Errors on Load Distribution and Tooth Load Sharing of Splines Under Combined Loading Conditions. *Journal of Mechanical Design*, 137(3), 032601.



- [19] Mărgineanu, D., Sticlaru, C., Davidescu, A., & Mărgineanu, E. (2017). Analytic and FEM Study of Load Distribution on the Length of Spline Joints Under Pure Torque. In *New Advances in Mechanisms, Mechanical Transmissions and Robotics* (pp. 69-76). Springer, Cham.
- [20] Cuffaro, V., Curà, F., & Mura, A. (2014). Test rig for spline couplings working in misaligned conditions. *Journal of Tribology*, 136(1), 011104.
- [21] Curà, F., & Mura, A. (2014). Experimental and theoretical investigation about reaction moments in misaligned splined couplings. *Mechanical Systems and Signal Processing*, 45(2), 504-512.
- [22] Curà, F., & Mura, A. (2013). Experimental procedure for the evaluation of tooth stiffness in spline coupling including angular misalignment. *Mechanical Systems and Signal Processing*, 40(2), 545-555.
- [23] Curà, F., Mura, A., & Adamo, F. (2017). Fatigue damage in spline couplings: numerical simulations and experimental validation. *Procedia Structural Integrity*, 5, 1326-1333.
- [24] Medina, S. (2002). Fretting Wear of Misaligned Spline Couplings. *Imperial College of Science, Technology and Medicine, PhD dissertation*
- [25] Medina, S., & Olver, A. V. (2002). An analysis of misaligned spline couplings. *Proceedings of the Institution of Mechanical Engineers, Part J: Journal of Engineering Tribology*, 216(5), 269-278.
- [26] Medina, S., and Olver, A.V., 2000, "Regimes of Contact in Spline Couplings," *Journal of Tribology*, vol. no. 124, pp. 351-357
- [27] Henriot, G. Accouplement a denture, SEIE
- [28] ISO 21771: 2007. Gears—Cylindrical involute gears and gear pairs—Concepts and geometry.